



HAL
open science

Olfactory learning promotes input-specific synaptic plasticity in adult-born neurons.

Gabriel Lepousez, Antoine Nissant, Alex K Bryant, Gilles Gheusi, Charles A Greer, Pierre-Marie Lledo

► **To cite this version:**

Gabriel Lepousez, Antoine Nissant, Alex K Bryant, Gilles Gheusi, Charles A Greer, et al.. Olfactory learning promotes input-specific synaptic plasticity in adult-born neurons.. Proceedings of the National Academy of Sciences of the United States of America, 2014, 111 (38), pp.13984-9. 10.1073/pnas.1404991111 . pasteur-01586992

HAL Id: pasteur-01586992

<https://pasteur.hal.science/pasteur-01586992>

Submitted on 13 Sep 2017

HAL is a multi-disciplinary open access archive for the deposit and dissemination of scientific research documents, whether they are published or not. The documents may come from teaching and research institutions in France or abroad, or from public or private research centers.

L'archive ouverte pluridisciplinaire **HAL**, est destinée au dépôt et à la diffusion de documents scientifiques de niveau recherche, publiés ou non, émanant des établissements d'enseignement et de recherche français ou étrangers, des laboratoires publics ou privés.



Distributed under a Creative Commons Attribution - NonCommercial - ShareAlike 4.0 International License

Olfactory learning promotes input-specific synaptic plasticity in adult-born neurons

Gabriel Lepousez^{a,b,1,2}, Antoine Nissant^{a,b,1}, Alex K. Bryant^{a,b}, Gilles Gheusi^{a,b,c}, Charles A. Greer^{d,e}, and Pierre-Marie Lledo^{a,b,2}

^aPerception and Memory Laboratory, Neuroscience Department, Institut Pasteur and ^bCentre National de la Recherche Scientifique Unité Mixte de Recherche 3571, F-75724 Paris, France; ^cLaboratory of Experimental and Comparative Ethology, University of Paris 13, Sorbonne Paris Cité, F-93430 Villetaneuse, France; and Departments of ^dNeurobiology and ^eNeurosurgery, Yale University School of Medicine, New Haven, CT 06520

Edited by Fred H. Gage, The Salk Institute for Biological Studies, San Diego, CA, and approved August 14, 2014 (received for review March 19, 2014)

The production of new neurons in the olfactory bulb (OB) through adulthood is a major mechanism of structural and functional plasticity underlying learning-induced circuit remodeling. The recruitment of adult-born OB neurons depends not only on sensory input but also on the context in which the olfactory stimulus is received. Among the multiple steps of adult neurogenesis, the integration and survival of adult-born neurons are both strongly influenced by olfactory learning. Conversely, optogenetic stimulation of adult-born neurons has been shown to specifically improve olfactory learning and long-term memory. However, the nature of the circuit and the synaptic mechanisms underlying this reciprocal influence are not yet known. Here, we showed that olfactory learning increases the spine density in a region-restricted manner along the dendritic tree of adult-born granule cells (GCs). Anatomical and electrophysiological analysis of adult-born GCs showed that olfactory learning promotes a remodeling of both excitatory and inhibitory inputs selectively in the deep dendritic domain. Circuit mapping revealed that the malleable dendritic portion of adult-born neurons receives excitatory inputs mostly from the regions of the olfactory cortex that project back to the OB. Finally, selective optogenetic stimulation of olfactory cortical projections to the OB showed that learning strengthens these inputs onto adult-born GCs. We conclude that learning promotes input-specific synaptic plasticity in adult-born neurons, which reinforces the top-down influence from the olfactory cortex to early stages of olfactory information processing.

sensory systems | inhibitory circuits | piriform cortex | cortico-bulbar projections | glutamate

Within the framework of Hebbian theory, information processing, learning, and memory all depend on dramatic changes in the synaptic weights throughout life. Recent progress in microscopy has extended this notion to structural synaptic plasticity, as synaptic networks were reported to be highly dynamic because of ongoing mechanisms that encompass synapse formation, stabilization, and elimination (1). Therefore, when studying synaptic plasticity today, one has to take into account both the functional and structural changes that lead to continuous remodeling of a given synaptic network.

Developing cortical networks are molded by experience or activity patterns during a “sensitive period” in development (2). Similarly, newly formed neurons in the adult olfactory bulb (OB) may be subject to plastic changes during a restricted time window after generation (3). Identifying the neural mechanisms and the nature of signals that trigger changes in developing and adult brain circuits during critical periods is a matter of intense debate (4). To address this fundamental question of circuit plasticity, we used the adult OB circuit, which receives about 30,000 new neurons per day in rodents, as a model system. As in embryonic cell development, adult-born neuron integration is under a strong selection process in which half of the young neuronal population is eliminated (5). Sensory experience might promote cell survival during a specific critical window, when new neurons receive synaptic inputs from preexisting circuits (6–9) and exhibit long-term

potentiation (LTP) (10). During this window, an odor-reward association task (but not a mere odor exposure) promotes cell survival (11, 12) and specific activation of adult-born neurons monitored through immediate early gene labeling (13, 14). As a result, olfactory memory is impaired when adult neurogenesis is compromised (13, 15). Conversely, the selective stimulation of adult-born neurons improves olfactory learning and memory (16), suggesting that these neurons are part of the olfactory memory engram (17). Although recent transsynaptic strategies have revealed the presynaptic connectivity of adult-born neurons (18, 19), little is known about how learning affects their structural and synaptic plasticity or which circuits and presynaptic cells are functionally recruited with them during associative learning. By demonstrating that olfactory learning triggers both selective structural rearrangements and changes in synaptic transmission onto adult-born neurons, this study represents a first attempt to link associative learning to functional plasticity of circuits endowed with adult neurogenesis.

Results

Region-Specific Changes in Spine Density of Adult-Born Neurons After Learning. Because a sensitive period to olfactory learning was found in maturing adult-born neurons of the mouse OB (i.e., between 18 and 35 d) (12), we examined whether discrimination learning could affect the structural synaptic plasticity during this period. Eighteen days following labeling of a cohort of newborn neurons with a GFP-expressing lentivirus, mice were trained in an olfactory discrimination learning task (olfactory learning group or OL, $n = 6$) (Fig. 1 *A* and *B*). Exposed daily to a pair of

Significance

The olfactory bulb (OB) receives newly born neurons through adulthood. This process constitutes another means, in addition to molecular or synaptic changes within individual neurons, by which the OB can make changes to its functional circuitry. In this study, we show that adult-born OB neurons display adaptive changes in response to the sensory context. In a restricted domain of the dendritic arbor of adult-born neurons, we found that structural and functional changes are strongest when olfactory cues are associated with a reward. Thus, the recruitment of adult-born neurons should be seen as a form of metaplasticity that strengthens long-range functional connectivity in the olfactory system during learning.

Author contributions: G.L., A.N., A.K.B., G.G., C.A.G., and P.-M.L. designed research, performed research, analyzed data, and wrote the paper.

The authors declare no conflict of interest.

This article is a PNAS Direct Submission.

¹G.L. and A.N. contributed equally to this work.

²To whom correspondence may be addressed. Email: gabriel.lepousez@pasteur.fr or pierre-marie.lledo@pasteur.fr.

This article contains supporting information online at www.pnas.org/lookup/suppl/doi:10.1073/pnas.1404991111/-DCSupplemental.

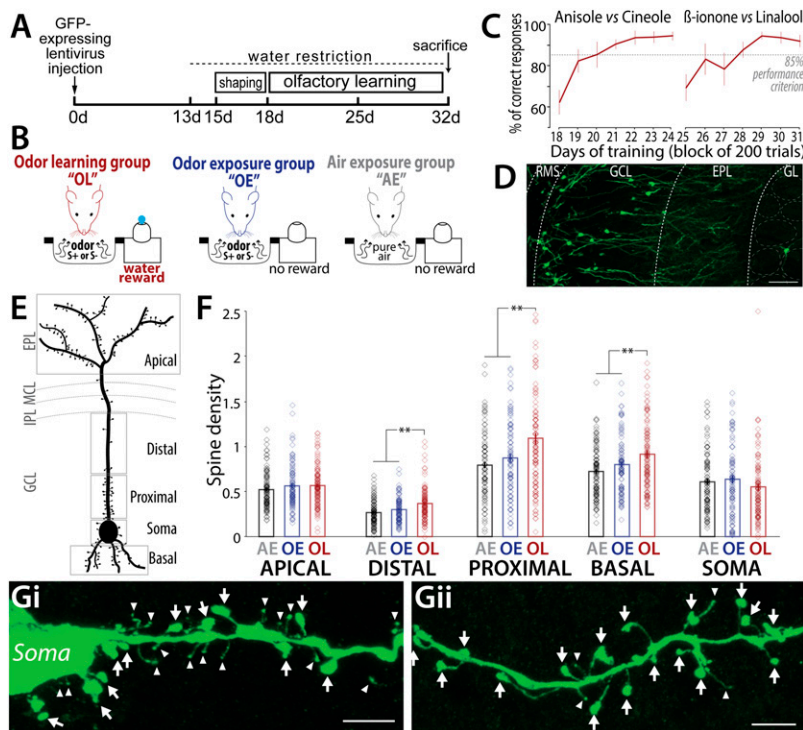


Fig. 1. Olfactory learning induced compartment-specific increase in spine density of adult-born GCs. (A) Experimental timeline. (B) Experimental groups. The OL (red) performed a discrimination learning task in which one odor of a pair was rewarded with water. The OE (blue) was exposed to the same odor presentation procedure without any reward contingency and received water at the end of the session. The AE (gray) was put in the same conditions as the OE group with the odor replaced by pure filtered air. (C) Daily odor discrimination performance of OL mice ($n = 6$). Mice were first trained to discriminate anisole versus cineole (1% in mineral oil) for the first week and β -ionone versus linalool (1%) for the second week. (D) GFP⁺ adult-born neurons at 32 dpi. Most adult-born neurons are GCs lying in the GCL with dendrites in the EPL. A few periglomerular cells in the GL are also visible. (Scale bar, 100 μ m.) (E) Schematic drawing of an adult-born GC and its different dendritic domains. (F) Spine-density histograms for each dendritic domain ($n = 95$ –100 dendritic segments analyzed from $n = 5$ –6 mice per condition). The somatic density is per 10 μ m², all other domains are per micrometer. **Bonferroni post hoc test, $P < 0.005$. Data are mean \pm SEM. (G) Adult-born GC spines in the somatic and proximal dendritic domains (i) and in the apical dendritic domain (ii), illustrating filipodia-like spines (arrowhead) and mushroom-like spines (arrow). (Scale bars, 5 μ m.)

odorants (200 trials per day for 14 d), OL mice gradually reached and exceeded the performance criterion of 85% of correct responses (Fig. 1C). As a control, one group of mice was exposed to the same olfactory stimulation procedure but did not receive reinforcement (odor-exposure group or OE, $n = 6$) (Fig. 1B). Meanwhile, another control group was exposed to purified air in the same context (air-exposure group or AE, $n = 5$) (Fig. 1B). By the end of the 14-d stimulation protocol, all animals were killed [age of GFP⁺ neurons, 29–35 d postinjection (dpi), hereafter called adult-born neurons; mean 32.1 ± 0.4 dpi, $n = 17$ mice] and GFP⁺ adult-born neurons with mature dendritic branching were observed preferentially in the granule cell layer (GCL; mean cell density, 97 ± 15 cells/mm²) and to a lesser extent in the glomerular layer (GL; mean cell density, 11 ± 2 cells/mm²) and the external plexiform layer (EPL; mean cell density, 2 ± 1 cell/mm²) (Fig. 1D), with only a negligible fraction of GFP⁺ cells expressing the immature marker polysialylated neuronal cell-adhesion molecule (PSA-NCAM; $6.3 \pm 3.5\%$, $n = 4$ mice).

We first characterized the synaptic structure and organization of adult-born GCs after olfactory learning, and subsequently in the two control groups. To quantify the spine density, GC dendritic trees were subdivided into five compartments: basal, somatic, proximal, distal, and apical domains (Fig. 1E). The proximal compartment was defined as the first 30 μ m of the main dendrite starting from the soma, the distal compartment as the adjacent segment starting 30 μ m away but still within the GCL, and the apical compartment as the dendritic arbor located in the EPL beginning at the first dendritic branch point (Fig. 1E). Our classification also relies on functional properties. Whereas the apical dendritic domain receives synaptic inputs from dendrites, axonal terminals exclusively contact the basal, somatic, proximal, and distal domains. We found that spine density was specifically increased after olfactory learning compared with the two control groups, in the distal [$F(\text{treatment})_{2, 317} = 11.0$, $P < 0.0001$; OL vs. AE, +36.3%; OL vs. OE, +22.1%; Bonferroni post hoc test, $P < 0.005$], proximal [$F_{2, 317} = 9.21$, $P = 0.0001$; OL vs. AE, +37.4%; OL vs. OE, +24.9%; $P < 0.005$], and basal domains ($F_{2, 317} = 7.27$, $P = 0.0008$; OL vs. AE, +26.7%; OL vs. OE, +15.6%; $P < 0.01$),

but not on the soma ($F_{2, 317} = 1.28$, $P = 0.277$) or in the apical compartment ($F_{2, 317} = 1.1$, $P = 0.333$) (Fig. 1F).

Dendritic spines could be divided into large-head mushroom-like spines and headless filipodia-like spines (Fig. 1G), the latter often considered as immature spines (20). The percentage of filipodia-like spines was variable across the dendritic subcompartments, with filipodia being significantly less dominant in the apical domain ($33.0 \pm 1.6\%$), intermediate in the basal domain ($40.0 \pm 1.7\%$), and enriched in the distal ($48.5 \pm 2.0\%$), proximal ($46.1 \pm 1.9\%$), and somatic domains [$47.9 \pm 2.0\%$; $F(\text{domain})_{4, 1566} = 28.64$, $P < 0.0001$]. This distribution was not affected by olfactory learning [$F(\text{domain} \times \text{treatment})_{4, 2} = 0.702$, $P = 0.69$; for each compartment, $F(\text{treatment})_{2, 317} < 2.9$, $P > 0.05$]. These data indicate that the dendritic regions displaying a higher density of immature spines were the most responsive to learning.

Both Excitatory and Inhibitory Inputs Increase After Learning. We next asked whether the observed compartment-specific changes in spine density were differentially associated with alterations in excitatory and inhibitory synaptic inputs. To selectively quantify adult-born GC glutamatergic inputs, PSD95, a postsynaptic scaffolding protein of glutamatergic synapses, was visualized using lentiviral expression of PSD95 fused to GFP (7, 8, 20–22). PSD95-GFP⁺ puncta were observed mainly in spine heads and, to a lesser degree, in the dendritic shafts (Fig. 2A). As was observed with GFP⁺ adult-born neurons, learning increased the PSD95-GFP⁺ spine density selectively in the distal [$F(\text{treatment})_{2, 119} = 3.42$, $P = 0.035$; OL vs. AE, +32.4%; Bonferroni post hoc test, $P < 0.01$], proximal ($F_{2, 120} = 6.82$, $P = 0.001$; OL vs. AE, +34.9%; OL vs. OE, +33.5%; $P < 0.003$), and basal compartments ($F_{2, 120} = 5.53$, $P = 0.005$; OL vs. AE, +31.9%; OL vs. OE, +30.4%; $P < 0.007$) (Fig. 2B). There was no significant effect of olfactory learning in the somatic ($F_{2, 120} = 2.21$, $P = 0.113$) and apical domains ($F_{2, 93} = 1.41$, $P = 0.248$), nor in the dendritic shaft compared with the two other treatments ($F_{2, 120} < 2.7$, $P > 0.07$ for all dendritic domains).

To analyze presumptive inhibitory inputs in GFP⁺ adult-born GCs, we quantified the presence of gephyrin, a postsynaptic protein essential for the clustering of GABA_A receptors. Gephyrin

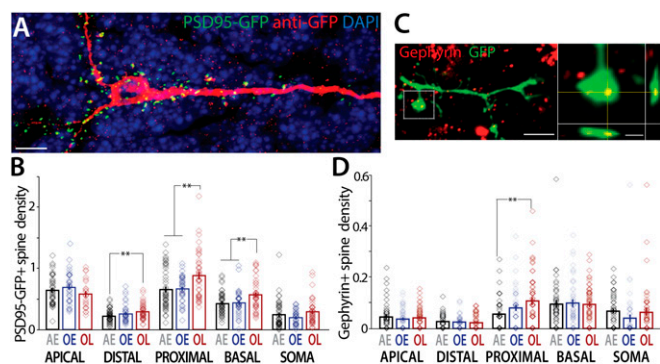


Fig. 2. Balance between excitatory and inhibitory synaptic inputs in adult-born GC. (A) PSD95-GFP⁺ adult-born GC, with PSD95-GFP⁺ puncta in green and dendritic morphology in red (anti-GFP). (Scale bar, 10 μm .) (B) Density of PSD95-GFP⁺ spines in the different dendritic domains ($n = 25\text{--}45$ dendritic segments per condition, $n = 9$ mice). The somatic density is per 10 μm^2 , all other domains are per micrometer. **Bonferroni post hoc test, $P < 0.01$. (C) Gephyrin-positive clusters (red) in GFP⁺ adult-born GC spines. (Scale bar, 5 μm .) (Right, Inset) Higher 3D magnification of the boxed region (Scale bar, 1 μm). (D) Density of gephyrin-positive spines in the different dendritic domains of GFP⁺ cells ($n = 45\text{--}50$ dendritic segments per condition, $n = 17$ mice). The somatic density is per 10 μm^2 , all other domains are per micrometer. **Bonferroni post hoc test, $P < 0.016$. Data are mean \pm SEM.

puncta colocalized with GFP were seen mainly in the dendritic shaft and in spine heads (Fig. 2C) [$92.6 \pm 1.8\%$ of gephyrin-positive spines are mushroom-like spines, without any significant difference between groups ($F_{2, 547} = 0.308$, $P = 0.734$)]. It is noteworthy, however, that the gephyrin staining in the apical domain might include a minor contribution from false-positives caused by GABAergic output of GCs onto mitral/tufted (M/T) cells. Olfactory learning increased the gephyrin-positive spine density specifically in the proximal domain ($F_{2, 156} = 5.1$, $P = 0.007$; OL vs. AE, +93.1%; Bonferroni post hoc test, $P = 0.0019$) (Fig. 2D) with no effect in the other domains ($F_{2, 156} < 2.1$, $P > 0.12$). This increase was also observed for the gephyrin puncta of the dendritic shaft in the proximal domain ($F_{2, 156} = 3.18$, $P = 0.044$; OL vs. AE, +34.1%; $P = 0.015$; others domains, $F_{2, 156} < 0.5$, $P > 0.6$). Collectively, these data showed that olfactory learning during a sensitive period of synaptic development led to compartment-defined modifications of the excitatory and inhibitory synapses that impinge onto adult-born GCs.

Learning Increases Excitatory Inputs from the Olfactory Cortex onto Newborn Neurons.

To identify the origin of the presynaptic inputs of adult-born GC spines, we selectively labeled the different glutamatergic cell populations that innervate the GCL. Anatomical and physiological studies have shown that the olfactory cortex (OC), notably the anterior piriform cortex (APC) and the anterior olfactory nucleus (AON), send dense projections back to the OB where they impinge notably onto GCs (18, 19, 23, 24). We injected an adeno-associated virus (AAV) expressing channelrhodopsin-2 (ChR2) fused to the red fluorescent protein mCherry into the APC and AON (Fig. 3A). One month later, ChR2-mCherry was present in axonal fibers with most of the labeling in the GCL, a lesser expression in the internal plexiform layer (IPL) and mitral cell layer (MCL) (Fig. 3A and B). Higher magnification confirms that labeled fibers and axonal boutons in the GCL were glutamatergic (Fig. 3C). Injection in the APC and AON did not significantly label M/T cells in a retrograde manner (2.2 ± 1.5 M/T-cells per section, $n = 6$ animals) nor did it significantly label migrating neuroblasts en route to the OB (0.32 ± 0.18 cell/ mm^2 in GCL, $n = 6$).

To estimate the ratio between OC (extrinsic) inputs and OB (intrinsic) inputs to new GCs, we made use of a transgenic mouse

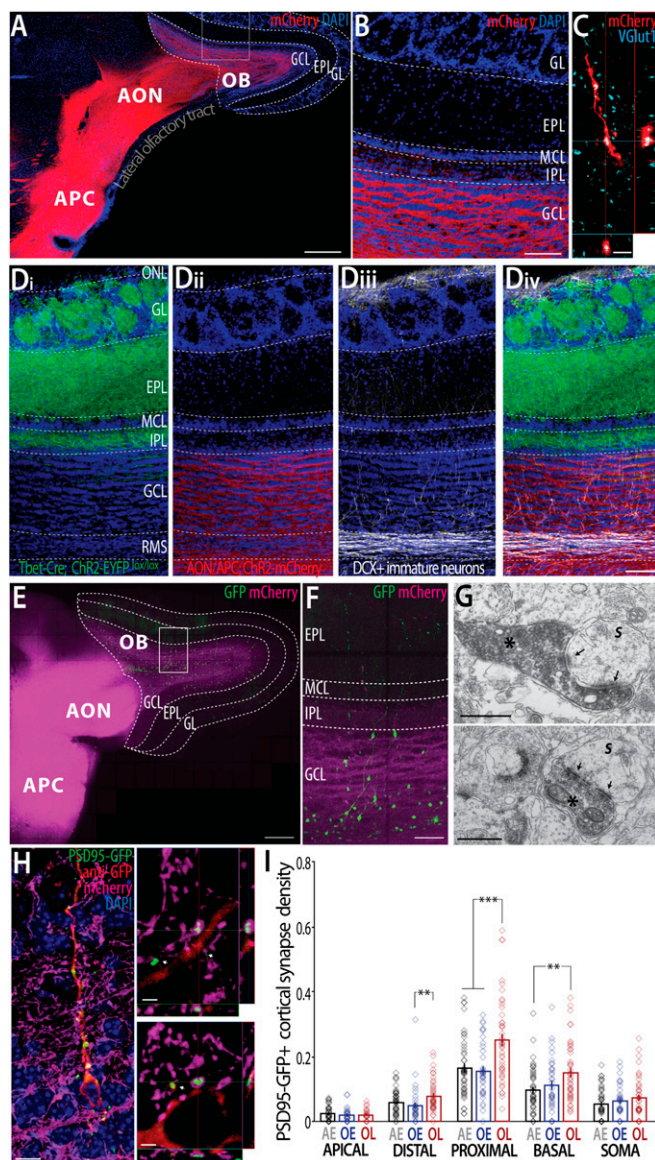


Fig. 3. Olfactory learning-induced remodeling of excitatory top-down inputs from the OC to adult-born GCs. (A) Transduction of the APC/AON with a Chr2-mCherry and the labeling of axonal projections to the OB. (Scale bar, 0.5 mm.) (B) Higher magnification showing the presence of cortico-bulbar axonal projections targeting the GCL and to a lesser extent the IPL and MCL. (Scale bar, 100 μm .) (C) Colocalization of VGlut1⁺ clusters (cyan) with mCherry⁺ fibers (red) in the GCL. (Scale bar, 1 μm .) (D) Conditional expression of Chr2-EYFP (green) in Cre-expressing M/T cells (*Tbet-cre* mice, $n = 3$ mice), Chr2-mCherry expression in cortico-bulbar projections (red), doublecortin⁺ immature adult-born neurons (white). (Scale bar, 100 μm .) (E and F) ChR2-mCherry⁺ cortico-bulbar projections (magenta) and GFP⁺ adult-born neurons (green) (Scale bars: 500 μm in E; 100 μm in F.) (G) Electron micrographs showing DAB-labeled mCherry⁺ cortical axon terminals in the GCL establishing typical type-1 asymmetric synapses onto a presumed spine (S). Arrow, postsynaptic density. (Scale bar, 0.5 μm .) (H) PSD95-GFP⁺ adult-born GC making putative synapses with mCherry⁺ (magenta) cortical axonal boutons. (Scale bar, 10 μm .) (Right) High 3D magnification showing a putative synapse between a cortical presynaptic terminal (magenta) colocalized and wrapped around a postsynaptic PSD95-GFP⁺ spine. Arrows indicate PSD95-GFP⁺ puncta empty of any labeled presynaptic boutons. (Scale bars, 2 μm .) (I) Density of PSD95-GFP⁺ cortical synapses in the different dendritic domains. ($n = 25\text{--}45$ dendritic segments analyzed per condition, $n = 9$ mice). The somatic density is per 10 μm^2 , all other domains are per micrometer. Bonferroni post hoc test, ** $P < 0.01$; *** $P < 0.001$. Data are mean \pm SEM. See also Fig. S1.

line (*Tbet-cre*) (25) that expresses Cre recombinase selectively in OB relay neurons. We injected an AAV in the OB to drive a Cre-dependent expression of ChR2-eYFP in relay neurons while a second AAV was injected in the OC to express ChR2-mCherry in cortical top-down fibers in the same hemisphere (Fig. 3*D* and Fig. S1). With this dual labeling, we observed a clear segregation of the excitatory inputs between the OB layers: the GL and EPL were almost exclusively filled with M/T-cell dendrites, whereas M/T-cell axon collaterals were found mainly in the IPL and more rarely in the GCL (Fig. 3*D*, *i*). In the ventral region, M/T-cell axons gathered into bundles of likely myelinated fibers before leaving to form the lateral olfactory tract. In contrast, cortical top-down axons were the dominant source of excitatory inputs to the GCL but not to other layers (Fig. 3*D*, *ii*). The IPL was the only region where both intrinsic and extrinsic fibers could be seen together (Fig. 3*D*, *iv*). We concluded that GC excitatory inputs within the GCL originated predominantly from extrinsic sources, mostly from the olfactory cortical areas.

Given that learning-induced synaptic changes were restricted to the dendritic domains in the GCL, we next sought to evaluate whether olfactory learning affected synaptic development of excitatory inputs from cortical top-down axons. To do so, we selectively labeled cortical fibers with ChR2-mCherry and newborn neurons with GFP (Fig. 3*E–G*) or PSD95-GFP (Fig. 3*H*). At 32 dpi, cortical top-down axonal boutons made putative synapses onto PSD95-GFP⁺ spines with presynaptic elements wrapping around the spines (Fig. 3*H*). Ultrastructural analysis with pre-embedding immunolabeling for mCherry confirmed that cortical axons in the GCL contained a large number of round vesicles and established typical asymmetrical contacts on spine-like structures with prominent postsynaptic densities, often exhibiting discontinuities (Fig. 3*H*). We next analyzed the distribution of excitatory cortical synapses throughout the dendritic tree (Fig. 3*H*). As expected, we found that the compartmental distribution of putative excitatory cortical synapses onto PSD95-GFP⁺ spines followed the pattern of cortical top-down innervation, with a higher density of cortical synapses in the basal, somatic, proximal, and distal compartments (percent of spines with a labeled presynaptic site: $24.1 \pm 1.3\%$, $22.8 \pm 1.8\%$, $23.7 \pm 0.8\%$, and $22.6 \pm 1.3\%$, respectively) and a negligible synapse density in the apical compartment ($2.7 \pm 0.3\%$). Olfactory learning led to a specific increase in cortical synapse density in the proximal ($F_{2, 120} = 10.22$, $P < 0.0001$; OL vs. OE, +59.8%; OL vs. AE, +53.9%; Bonferroni post hoc test, $P < 0.0002$) (Fig. 3*I*), distal ($F_{2, 119} = 4.18$, $P = 0.017$; OL vs. OE, +61.2%, $P = 0.006$; OL vs. AE, +33.8%, $P = 0.055$), and basal domains ($F_{2, 120} = 4.99$, $P = 0.008$; OL vs. AE, +54.6%, $P = 0.003$; OL vs. OE, +36.3%, $P = 0.032$), but had no effect on other compartments (for each domain, $F_{2, 93-120} < 1.1$, $P > 0.33$). Moreover, the proportion of excitatory cortical synapses within all of the PSD95-GFP⁺ spines increased selectively after learning in the proximal ($F_{2, 120} = 4.83$, $P = 0.009$; OL vs. AE, +20.5%; OL vs. OE, +27.3%, $P < 0.016$) and distal domains ($F_{2, 119} = 4.85$, $P = 0.009$; OL vs. OE, +48.3%, $P = 0.002$), but not other domains ($F_{2, 93-120} < 1.24$, $P > 0.29$). We conclude that learning induced a selective increase of excitatory inputs originating from the OC.

Learning Strengthens the Synaptic Transmission from the OC to Newborn Neurons. To probe the functional correlates of these morphological changes, we performed whole-cell patch-clamp recordings on 71 GFP⁺ adult-born GCs from the three experimental groups. Measurements of intrinsic membrane properties did not reveal differences in cell membrane capacitance, input membrane resistance, or density of voltage-dependent sodium current between the groups (Fig. S2). To assess the degree of synaptic activity, we recorded spontaneous inhibitory and excitatory postsynaptic currents (sIPSCs and sEPSCs, respectively). Amplitude and kinetics of sIPSCs were similar for all groups, but the frequency was significantly higher in the OL group (OL vs. OE: $P = 0.018$ with

a Mann–Whitney test) (Fig. 4*A* and Fig. S2). In contrast, the amplitude, frequency, and kinetics of sEPSCs did not significantly differ across the groups (Fig. 4*B* and Fig. S1). The majority of the recorded cells exhibited only large and sharp sEPSCs (Fig. 4 and Fig. S1), indicative of inputs from axon collaterals in the GCL but not from distant dendritic inputs in the EPL (26). Given that cortical top-down axons were the dominant source of excitatory axonal inputs to adult-born neurons in the GCL, we further characterized excitatory cortical inputs onto GCs using photoactivation of ChR2⁺ axons originating from AON/APC pyramidal cells to evoke EPSCs (Fig. 5*A*). By gradually increasing the duration of the light pulses (delivered at 0.2 Hz), we collected minimal (30–70% failures) and maximal responses (near 100% success with no further increase of the mean peak amplitude by increasing light duration) (Fig. 5*B*). The ratio between minimal and maximal responses ranged from 1 to 5.7 (mean: 2.4 ± 0.2 ; $n = 30$) and was similar for all groups (Fig. 5*C*). Interestingly, the amplitude of minimal EPSCs was increased in the OL group (AE vs. OL: $P = 0.022$ with Mann–Whitney test) (Fig. 5*D*), but the paired-pulse ratio (PPR) measured by delivering two light pulses (interpulse interval = 50 ms) was unchanged between groups (Fig. 5*E*), suggesting no modification in the probability of glutamate release. From these experiments, we conclude that olfactory learning increases the excitatory drive from the OC onto adult-born GCs.

Discussion

We have shown that olfactory learning enhances the density of dendritic spines in restricted domains of adult-born GCs, affecting both excitatory and inhibitory inputs. Using genetic labeling, we found that the most plastic dendritic domains of adult-born neurons were those that receive dense excitatory inputs from olfactory cortical regions. Optogenetic stimulation of these axon terminals revealed that learning strengthens the top-down excitatory drive from the OC onto adult-born GCs. Our data demonstrate that olfactory learning, by means of adult neurogenesis, triggers synapse-specific structural and functional plasticity, which reinforces synaptic connections between the OC and the OB.

Adult-Born GCs Display Experience-Dependent Structural Plasticity. It is well established that the GCL receives a mixture of intrinsic M/T-cell axon collaterals and extrinsic centrifugal axon terminals originating from cortical and subcortical regions. Using conditional genetic labeling, we demonstrated that intrinsic glutamatergic inputs and cortico-bulbar projections from the AON/APC are spatially segregated. This anatomical feature indicates that cells and dendrites in the GCL receive extrinsic cortical

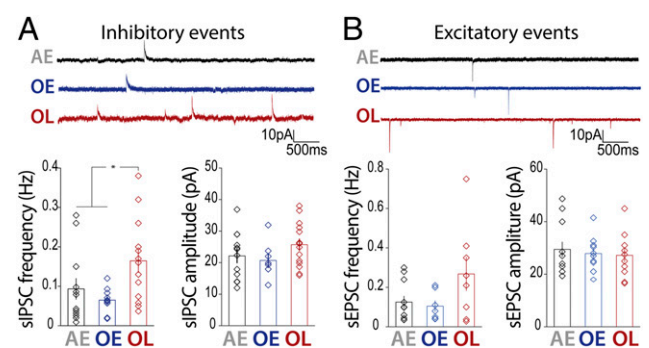


Fig. 4. Spontaneous inhibitory and excitatory synaptic events onto adult-born GCs. (*A*, *Upper*) Traces showing spontaneous IPSCs ($V_c = 0$ mV). (*Lower*) sIPSC frequency (Hz, *Left*) and sIPSC amplitude (pA, *Right*). (*B*, *Upper*) Traces showing spontaneous EPSCs ($V_c = -70$ mV). (*Lower*) sEPSC frequency (Hz, *Left*) and sEPSC amplitude (pA, *Right*). * $P < 0.05$ with Mann–Whitney test. Data are mean \pm SEM. See also Fig. S2.

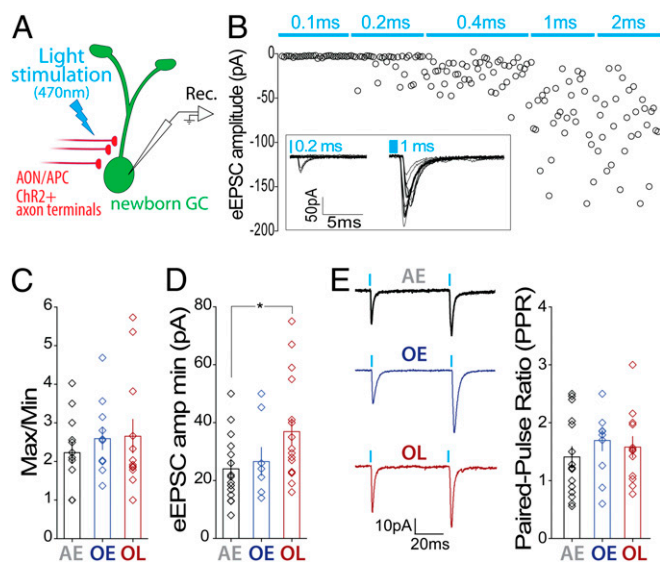


Fig. 5. Learning-induced enhancement of excitatory cortical top-down inputs onto adult-born GCs. (A) Evoked EPSC recording configuration during light stimulation of ChR2-expressing cortical top-down inputs from the APC/AON. (B) Amplitude of light evoked EPSCs (recorded at $V_c = -70$ mV) with respect to the light pulse duration (in milliseconds). (Inset) Superimposed traces in the 0.2-ms minimal stimulation condition (Left) and 2-ms stimulation condition (Right), illustrating the high failure rate and the similar amplitude of success responses during minimal stimulation. (C) Ratio between maximal and minimal evoked EPSCs. (D) Amplitude of minimal evoked EPSCs (pA). (E, Left) Minimal evoked EPSCs with paired-light stimulation (averaged from >30 individual EPSC; including failures; light-pulse duration, 0.2 ms; interspike interval, 50 ms). (Right) PPR (PPR = Amp2/Amp1). * $P < 0.05$ with Mann-Whitney test. Data are mean \pm SEM. See also Fig. S2.

inputs, whereas the IPL and the EPL are targeted by intrinsic M/T-cell inputs (see also ref. 21). The precise location of extrinsic excitatory inputs near the soma may make the cortico-bulbar inputs more likely to trigger action potentials (27). This feature is particularly relevant for adult-born neurons that are more excitable (6, 10) and preferentially activated by odorant stimuli (13, 14).

In this study, we show that discrimination learning increases excitatory inputs onto adult-born GCs specifically in the deep dendritic domains in the GCL but does not affect the apical domain corresponding to the dendrodendritic reciprocal synapse. Developmental analysis of apical spine density in adult-born GCs has shown a progressive increase at 15–30 dpi followed by a slight decrease and stabilization at 50–90 d (28–30). Olfactory deprivation between 15 and 30 dpi strongly reduces apical spine density (22), whereas passive odorant exposure has no significant effect on spine density (29) but decreases spine turnover (8). We also confirmed that neither odor exposure nor odor learning affects apical spine density and maturation, suggesting that apical spine turnover, rather than the total number of spines, is impacted by sensory experience. Conversely, we found that olfactory learning selectively increases spine density in the deep dendritic domains, where spines first appear before apical development (28). Spine density in the proximal compartment of adult-born GCs peaks at 15–30 d before further pruning at 90 dpi (29). Moreover, impairing NMDA receptors decreases the proximal spine density but sensory deprivation distinctly alters proximal and basal domains (22, 31). Collectively, these data indicate that sensory experience strongly influences the direction and location of structural synaptic plasticity.

Olfactory Learning Modifies Functional Synaptic Inputs onto Adult-Born GCs. Our slice recordings revealed a slight but insignificant increase in sEPSC frequency with no change in amplitude.

Spontaneous EPSCs consist of a heterogeneous population of synaptic events originating from cortical axons and from M/T-cell collaterals. Thus, learning-induced changes in cortical axon sEPSCs are intermingled with M/T-cell inputs, preventing further insight into the possible input-specific effects of learning using sEPSCs. We therefore developed an optogenetic strategy to analyze cortical excitatory inputs. Optogenetic stimulation of cortical axons contacting adult-born GCs revealed that the amplitude of minimal light-evoked responses was higher after learning. Further studies should investigate whether similar changes also occur on M/T-cell inputs. Combining this observation with the unchanged paired-pulse ratio suggests a postsynaptic locus for the learning-induced plasticity. This strengthening of cortical synapses might reflect a form of LTP, which might correlate with the increase in mature PSD95-containing spines seen after learning. This form of structural and synaptic plasticity could result from the activation of the glutamatergic signaling pathway (1). Alternatively, it could come from the action of neuromodulators, such as serotonin, acetylcholine, or noradrenaline, which may also be released during learning (32). Further experiments are needed to test whether olfactory learning occludes the induction of LTP in maturing GCs (10, 33) and to characterize the network activity, as well as the signaling pathway involved in learning-induced LTP.

The increase in minimal evoked EPSC amplitude was associated with a slight but not significant increase in the maximum/minimum ratio. This ratio—ranging from 1 to 5.7—does not correspond with either the density of the AON/APC synapses or the learning-induced increase. This discrepancy might be caused by the existence of a large proportion of silent synapses. However, it might simply reflect the experimental limitation that prevents us from activating all synapses because of our recording/stimulation conditions.

In addition to glutamatergic inputs, GCs also receive inhibitory inputs from local OB interneurons, called deep short-axon cells (34). These interneurons also receive cortico-bulbar inputs and thus provide disynaptic feed-forward inhibition onto GCs (23, 24). Adult-born neurons receive increasing numbers of functional inhibitory inputs during their maturation (29). Here, to our knowledge, we report for the first time an increase in putative gephyrin-positive puncta (both on spine and shaft) in the proximal domain following learning. Moreover, we found that adult-born GCs in the learning group received more frequent spontaneous inhibitory inputs—but their amplitudes remained constant—consistent with the higher number of inhibitory gephyrin-positive synapses in new GCs. This increase in inhibitory inputs could arise from different origins: (i) a simultaneous potentiation of cortical glutamatergic inputs on presynaptic inhibitory interneurons, changing their intrinsic excitability and increasing GABAergic synaptic transmission, as observed for hippocampal interneurons (35); and (ii) a maintenance of intrinsic excitation/inhibition balance to compensate for the changes in excitatory inputs, as observed in the cortex (36). Indeed, both excitatory and inhibitory inputs of the proximal domain increased after learning. However, this increase was not found in the other dendritic domains, suggesting a potential reorganization of the cell excitation/inhibition balance after learning. The excitation/inhibition balance is important for action potential generation, dendritic propagation, and spike-timing precision, as shown in the adult-born GCs of the dentate gyrus (37).

Strengthening the Cortical Top-Down Projections into the OB. Olfactory learning consistently led to a strong significant increase in both spine density and synaptic transmission, whereas olfactory exposure showed a weak and nonsignificant increase compared with air exposure. These results suggest that olfactory learning has a significant additive effect compared with passive sensory exposure, which may represent the activation of circuits linked with associative and mnemonic processes in the OC (38). Further

studies are needed to decipher whether this effect concerns the entire population of GCs or only adult-born GCs during a sensitive period of development. Importantly, the olfactory learning task engages additional cognitive processes, such as vigilance, motivation, and anticipation, which may be transmitted to the OB via cortical top-down or neuromodulatory inputs and may contribute to the strong effect observed after learning.

What is the nature of the message transmitted by top-down cortical projections onto GCs? In vivo recordings in freely behaving animals during a discrimination task revealed that odor-evoked APC pyramidal cell activity is rather sparse and phase-locked to the sniff cycle. These cells convey information both on odor identity and odor value and their activity evolve after learning (38, 39). This observation suggests that top-down cortical projections transmit higher-order attributes to the OB circuit, such as valence and memory-related features. Interestingly, learning to associate odorant cues with a reward evokes coherent β -oscillations (15–40 Hz) between the APC and OB (40). This long-range β -synchronization process is selectively impaired after lesioning the cortico-bulbar inputs (40), suggesting that GCs receive synchronous top-down cortical inputs in the β -range during learning. Synchronized top-down cortical inputs to the OB are also observed during slow-wave sleep, a physiological state during which adult-born cell death has been reported (41). At the cellular level, cortical excitatory inputs onto GCs exhibit LTP (10, 33), a feature that can ultimately facilitate GC spiking and promote feed-forward inhibition onto M/T cells (33). This feed-forward inhibition may participate in gain control of odor-evoked responses in M/T cells, as observed when it is mimicked by optogenetic activation of adult-born GCs, specifically in the

β -frequency (16). In addition, this top-down feed-forward inhibition could help synchronize distant M/T cells, thereby facilitating the bottom-up flow of information to the OC pyramidal cells by increasing input coincidence. Further characterization of the cortico-bulbar activity during odor learning and direct testing of how it can affect structural and synaptic plasticity will be needed to fully understand the circuit basis of the olfactory engram.

Materials and Methods

Stereotaxic Viral Injections. The rAAV-hSyn-ChR2(H134R)-mCherry-WPRE was injected in the AON/APC and the LV-CMV-GFP-WPRE or LV-EF1a-PSD95-GFP-WPRE were injected in the RMS.

Behavior. Olfactory stimulation was performed as described in ref. 16.

Electrophysiology. Adult-born cell recordings were performed as described in ref. 10.

Immunohistochemistry, Electron Microscopy, and Image Analysis. Optimal detection and quantification of postsynaptic markers and pre-embedding electron micrographs were obtained as described previously (29). See *SI Materials and Methods* for more detailed information.

ACKNOWLEDGMENTS. We thank Laura Benoit for her technical help; all members of the P.-M.L. laboratory for their insights; Anne Lanjuin and Catherine Dulac for providing us with the *Tbet-Cre* mice; Yoav Livneh and Adi Mizrahi for the PSD95-GFP construct; and Karl Deisseroth for the ChR2 construct. The P.-M.L. laboratory is part of the École des Neurosciences de Paris network and member of the Laboratoire d'Excellence Revive (ANR-10-LABX-73). This work was supported by the life insurance company "AG2R-La-Mondiale" and Agence Nationale de la Recherche (ANR-BLAN-SVSE4-LS-110624).

- Holtmaat A, Svoboda K (2009) Experience-dependent structural synaptic plasticity in the mammalian brain. *Nat Rev Neurosci* 10(9):647–658.
- Hensch TK (2005) Critical period plasticity in local cortical circuits. *Nat Rev Neurosci* 6(11):877–888.
- Yamaguchi M, Mori K (2005) Critical period for sensory experience-dependent survival of newly generated granule cells in the adult mouse olfactory bulb. *Proc Natl Acad Sci USA* 102(27):9697–9702.
- Toyoizumi T, et al. (2013) A theory of the transition to critical period plasticity: Inhibition selectively suppresses spontaneous activity. *Neuron* 80(1):51–63.
- Petreanu L, Alvarez-Buylla A (2002) Maturation and death of adult-born olfactory bulb granule neurons: role of olfaction. *J Neurosci* 22(14):6106–6113.
- Carleton A, Petreanu LT, Lansford R, Alvarez-Buylla A, Lledo P-M (2003) Becoming a new neuron in the adult olfactory bulb. *Nat Neurosci* 6(5):507–518.
- Kelsch W, Lin C-W, Lois C (2008) Sequential development of synapses in dendritic domains during adult neurogenesis. *Proc Natl Acad Sci USA* 105(43):16803–16808.
- Livneh Y, Mizrahi A (2012) Experience-dependent plasticity of mature adult-born neurons. *Nat Neurosci* 15(1):26–28.
- Katagiri H, et al. (2011) Dynamic development of the first synapse impinging on adult-born neurons in the olfactory bulb circuit. *Neural Syst Circuits* 1(1):6.
- Nissant A, Bardy C, Katagiri H, Murray K, Lledo PM (2009) Adult neurogenesis promotes synaptic plasticity in the olfactory bulb. *Nat Neurosci* 12(6):728–730.
- Alonso M, et al. (2006) Olfactory discrimination learning increases the survival of adult-born neurons in the olfactory bulb. *J Neurosci* 26(41):10508–10513.
- Mouret A, et al. (2008) Learning and survival of newly generated neurons: When time matters. *J Neurosci* 28(45):11511–11516.
- Moreno MM, et al. (2009) Olfactory perceptual learning requires adult neurogenesis. *Proc Natl Acad Sci USA* 106(42):17980–17985.
- Belnoue L, Grosjean N, Abrus DN, Koehl M (2011) A critical time window for the recruitment of bulbar newborn neurons by olfactory discrimination learning. *J Neurosci* 31(3):1010–1016.
- Lazarini F, et al. (2009) Cellular and behavioral effects of cranial irradiation of the subventricular zone in adult mice. *PLoS ONE* 4(9):e7017.
- Alonso M, et al. (2012) Activation of adult-born neurons facilitates learning and memory. *Nat Neurosci* 15(6):897–904.
- Lepousez G, Valley MT, Lledo P-M (2013) The impact of adult neurogenesis on olfactory bulb circuits and computations. *Annu Rev Physiol* 75:339–363.
- Arenkiel BR, et al. (2011) Activity-induced remodeling of olfactory bulb microcircuits revealed by monosynaptic tracing. *PLoS ONE* 6(12):e29423.
- Deshpande A, et al. (2013) Retrograde monosynaptic tracing reveals the temporal evolution of inputs onto new neurons in the adult dentate gyrus and olfactory bulb. *Proc Natl Acad Sci USA* 110(12):E1152–E1161.
- Cane M, Maco B, Knott G, Holtmaat A (2014) The relationship between PSD-95 clustering and spine stability in vivo. *J Neurosci* 34(6):2075–2086.
- Livneh Y, Feinstein N, Klein M, Mizrahi A (2009) Sensory input enhances synaptogenesis of adult-born neurons. *J Neurosci* 29(1):86–97.
- Kelsch W, Lin CW, Mosley CP, Lois C (2009) A critical period for activity-dependent synaptic development during olfactory bulb adult neurogenesis. *J Neurosci* 29(38):11852–11858.
- Boyd AM, Sturgill JF, Poo C, Isaacson JS (2012) Cortical feedback control of olfactory bulb circuits. *Neuron* 76(6):1161–1174.
- Markopoulos F, Rokni D, Gire DH, Murthy VN (2012) Functional properties of cortical feedback projections to the olfactory bulb. *Neuron* 76(6):1175–1188.
- Haddad R, et al. (2013) Olfactory cortical neurons read out a relative time code in the olfactory bulb. *Nat Neurosci* 16(7):949–957.
- Schoppa NE (2006) AMPA/kainate receptors drive rapid output and precise synchrony in olfactory bulb granule cells. *J Neurosci* 26(50):12996–13006.
- Egger V, Svoboda K, Mainen ZF (2005) Dendrodendritic synaptic signals in olfactory bulb granule cells: Local spine boost and global low-threshold spike. *J Neurosci* 25(14):3521–3530.
- Whitman MC, Greer CA (2007) Synaptic integration of adult-generated olfactory bulb granule cells: Basal axodendritic centrifugal input precedes apical dendrodendritic local circuits. *J Neurosci* 27(37):9951–9961.
- Palotto M, et al. (2012) Early formation of GABAergic synapses governs the development of adult-born neurons in the olfactory bulb. *J Neurosci* 32(26):9103–9115.
- Breton-Provencher V, Coté D, Saghatelian A (2014) Activity of the principal cells of the olfactory bulb promotes a structural dynamic on the distal dendrites of immature adult-born granule cells via activation of NMDA receptors. *J Neurosci* 34(5):1748–1759.
- Kelsch W, Li Z, Eliava M, Goenrich C, Monyer H (2012) GluN2B-containing NMDA receptors promote wiring of adult-born neurons into olfactory bulb circuits. *J Neurosci* 32(36):12603–12611.
- Mouret A, Murray K, Lledo P-M (2009) Centrifugal drive onto local inhibitory interneurons of the olfactory bulb. *Ann N Y Acad Sci* 1170:239–254.
- Gao Y, Strowbridge BW (2009) Long-term plasticity of excitatory inputs to granule cells in the rat olfactory bulb. *Nat Neurosci* 12(6):731–733.
- Eyre MD, Antal M, Nusser Z (2008) Distinct deep short-axon cell subtypes of the main olfactory bulb provide novel intrabulbar and extrabulbar GABAergic connections. *J Neurosci* 28(33):8217–8229.
- Campanac E, et al. (2013) Enhanced intrinsic excitability in basket cells maintains excitatory-inhibitory balance in hippocampal circuits. *Neuron* 77(4):712–722.
- House DRC, Elstrott J, Koh E, Chung J, Feldman DE (2011) Parallel regulation of feed-forward inhibition and excitation during whisker map plasticity. *Neuron* 72(5):819–831.
- Marin-Burgin A, Mongiat LA, Pardi MB, Schinder AF (2012) Unique processing during a period of high excitation/inhibition balance in adult-born neurons. *Science* 335(6073):1238–1242.
- Wilson DA, Sullivan RM (2011) Cortical processing of odor objects. *Neuron* 72(4):506–519.
- Gire DH, Whitesell JD, Doucette W, Restrepo D (2013) Information for decision-making and stimulus identification is multiplexed in sensory cortex. *Nat Neurosci* 16(8):991–993.
- Martin C, Gervais R, Messaoudi B, Ravel N (2006) Learning-induced oscillatory activities correlated to odour recognition: A network activity. *Eur J Neurosci* 23(7):1801–1810.
- Yokoyama TK, et al. (2011) Elimination of adult-born neurons in the olfactory bulb is promoted during the postprandial period. *Neuron* 71(5):883–897.